Vehicle longitudinal and lateral velocity estimation with nonlinear observers

Marcus Engebretsen[1]

***Abstract*—Precise knowledge of velocities is essential in low level torque allocation algorithms for race car driving. Velocity estimation is therefore essential in the absence of direct velocity measurements. This paper compares two high performance velocity observers in the CarMaker simulation environment on a Formula Student race car. The approaches comprises a regular nonlinear observer and a sliding mode observer (SMO).**

I. INTRODUCTION

Estimation of friction forces in the setting of race car driving is a highly nonlinear challenge. *Driving a car as fast as possible (in a race) is all about maintaining the highest possible acceleration level in the appropriate direction* [1]. Producing any useful results using nominal estimation techniques therefore requires the ability to observe and model fast dynamics. In this work the problem of estimating longitudinal and lateral velocity has been approached using nonlinear observers.

Nonlinear observers are computationally efficient tools that doesn't require much strain to implement. In [2] an input to state stable (ISS) nonlinear observer for longitudinal and lateral velocity is presented. This observer is reused in [3], extended with an adaptive update law that estimates the wheel-road friction parameter. The results from both these approaches show promise due to the extensive testing with a vehicle operating with large accelerations and the nonlinear stability analysis performed in [2]. Another promising estimator that is frequently proposed as a solution to vehicle velocity estimation is the SMO, see e.g. [4], [5], [6]. There exists stability proofs for this approach as well, showing similar results as in [2], see e.g. [6].

The two aforementioned approaches have been implemented for comparison in a simulation environment for a Formula Student race car. The intention is to estimate longitudinal and lateral velocities at a high rate for the torque allocation control system as a redundant option in case of absent GPS data.

A difficulty with implementing both these observer techniques is that they require accurate estimates of the longitudinal and lateral wheel forces. These forces can be obtained using the steady-state Pacejka wheel-model [7], known as the magic formula, provided that the parameters of the model are identified correctly.

This paper is organized by first presenting the magic formula along with the definitions for side slip angles and slip ratios in Section (II). Subsequently the kinematic model for the velocity dynamics are presented along with the ISS nonlinear observer and the SMO in Section (III). To compare the two approaches the essential parts of their stability analysis is discussed in Section (IV). Lastly simulation results from CarMaker are shown in Section (V).

II. WHEEL MODELING

Parameters	Description
l_r	Rear axle length (m)
l_f	Front axle length (m)
l_w	Wheelbase length (m)
m	Vehicle mass (kg)
I_z	Moment of inertia yaw axis (kgm^2)

The wheel forces are calculated based on a simplified steady-state Pacejka model that depends on the side slip angles and the slip ratios of each wheel. The side slip angles are calculated according to the equations

$$\begin{aligned} SA_{FL} &= \arctan\left(\frac{v_y + l_f r}{v_x + \frac{l_w}{2} r}\right) \\ SA_{FR} &= \arctan\left(\frac{v_y + l_f r}{v_x - \frac{l_w}{2} r}\right) \\ SA_{RL} &= \arctan\left(\frac{v_y - l_r r}{v_x + \frac{l_w}{2} r}\right) \\ SA_{RR} &= \arctan\left(\frac{v_y - l_r r}{v_x - \frac{l_w}{2} r}\right) \end{aligned} \tag{1}$$

where v_x is longitudinal velocity, v_y is lateral velocity and r is the yaw rate. These equations describe how each wheel slips laterally when the car turns. The slip ratios are consequently defined according to

$$\begin{aligned} SR_{FL} &= \frac{\omega_{FL} R_{FL}^{eff} - v_x + \frac{l_w}{2} r}{v_x - \frac{l_w}{2} r} \\ SR_{FR} &= \frac{\omega_{FL} R_{FL}^{eff} - v_x - \frac{l_w}{2} r}{v_x + \frac{l_w}{2} r} \\ SR_{RL} &= \frac{\omega_{FL} R_{FL}^{eff} - v_x + \frac{l_w}{2} r}{v_x - \frac{l_w}{2} r} \\ SR_{RR} &= \frac{\omega_{FL} R_{FL}^{eff} - v_x - \frac{l_w}{2} r}{v_x + \frac{l_w}{2} r} \end{aligned} \tag{2}$$

where ω_i is the wheel angular velocity and R_i^{eff} is the wheel effective radius. The slip ratio describes to what extent the wheel slips in the longitudinal direction. It depends on a relationship between rolling speed of each wheel and the longitudinal velocity, Equation (2). For a more elaborate description of these concepts, see e.g. [1].

The magic formula can be defined for longitudinal and lateral wheel forces for each wheel assuming knowledge of Equations (1) and (2), see [7].

$$
\begin{aligned}
F_{x,i} &= D_{x,i} \sin\Big(C_x \arctan\Big(B_x SA_i - E_x\Big(B_x SA_i - \arctan\Big(B_x SA_i\Big)\Big)\Big)\Big) \\
F_{y,i} &= D_{y,i} \sin\Big(C_y \arctan\Big(B_y SR_i - E_t\Big(B_y SR_i - \arctan\Big(B_y SR_i\Big)\Big)\Big)\Big)
\end{aligned} \tag{3}
$$

where $i \in \{FL,FR,RL,RR\}$. Assumptions done in Equation (3) are

- All wheels are identical.
- All wheels experience equivalent surface conditions.

It is important to note that these assumptions render the parameters B_j, C_j and E_j for $j \in \{x, y\}$ equal for each wheel. The $D_{j,i}$'s on the other hand are functions of the normal load exerted on the wheels along with the maximal friction coefficient, see [7]. This dependence makes it a time-varying parameter. It is further assumed that the normal force on each wheel is known from hard physical modelling of the vehicle dynamics. The exact modeling and estimation of these forces exceeds the scope of this work.

To summarize, calculating wheel forces depends on knowledge of the exogenous signals

- Wheel speeds: $\omega_{FL}, \omega_{FR}, \omega_{RL}$ and ω_{RR}
- Effective wheel radii: R^{eff}_{FL}, R^{eff}_{FR}, R^{eff}_{RL} and R^{eff}_{RR}
- Normal forces: $F_{z,FL}, F_{z,FR}, F_{z,RL}$ and $F_{z,RR}$
- Yaw rate: r
- Velocities: v_x and v_y.

where the wheel speeds and the yaw rate originate from sensor measurements. The effective radii are assumed calculated in the same fashion as the normal forces through hard physical modelling. It is known that the estimated forces resulting from Equation (3) are time-varying. However notation will be abused in this paper for simplicity, denoting the forces without time dependence.

III. Vehicle modelling

An illustration of the vehicle is shown in Figure (1). The vehicle is modelled using a 3-DOF model including longitudinal velocity, lateral velocity and yaw rate, $x = (v_x, v_y, r)$

$$
\begin{bmatrix} \dot{v}_x \\ \dot{v}_y \\ \dot{r} \end{bmatrix} = \begin{bmatrix} v_y r + a_x \\ -v_x r + a_y \\ \frac{1}{I_z} \sum M_z \end{bmatrix} \tag{4}
$$

where $\sum M_z$ is defined in Appendix (VI-A). The equations for $\dot{v}_x$ and $\dot{v}_y$ are both based on linear accelerations and Coriolis terms acting through the center of gravity, see Figure (1).

The observer proposed in [2] is

$$
\begin{bmatrix} \dot{\hat{v}}_x \\ \dot{\hat{v}}_y \\ \dot{\hat{r}} \end{bmatrix} = \begin{bmatrix} \hat{v}_y r + a_x + \sum_i K_i (v_{x,i} - \hat{v}_x) \\ -\hat{v}_x r + a_y - K_y (a_y - \frac{1}{m} \sum \hat{F}_y) \\ \frac{1}{I_z} \sum \hat{M}_z + K_r (r - \hat{r}) \end{bmatrix} \tag{5}
$$

where $i \in \{FL,FR,RL,RR\}$, $\sum F_y$ is defined in Appendix (VI-A) and $v_{x,i}$ is defined in Appendix (VI-B). This observer is compared to a modified version of the SMO proposed in [6]

$$
\begin{bmatrix} \dot{\hat{v}}_x \\ \dot{\hat{v}}_y \\ \dot{\hat{r}} \end{bmatrix} = \begin{bmatrix} \hat{v}_y r + a_x + \sum_i K_i (v_{x,i} - \hat{v}_x) \\ -\hat{v}_x r + a_y - l_y (a_y - \frac{1}{m} \sum \hat{F}_y) - \rho_y \operatorname{sgn}(a_y - \frac{1}{m} \sum \hat{F}_y) \\ \frac{1}{I_z} \sum \hat{M}_z + l_r (r - \hat{r}) + \rho_r \operatorname{sgn}(r - \hat{r}) \end{bmatrix} \tag{6}
$$

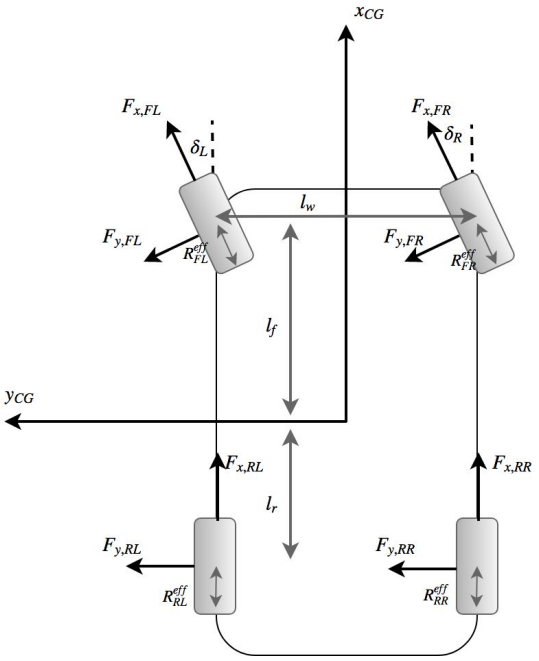

Fig. 1. Illustration of the vehicle model.

The part of the observer estimating v_x is changed from the original proposal in [6] to be equivalent to that of Equation (5). This is to obtain a better comparison of lateral velocity estimates between the two methods. For easy comparison with the observer in Equation (5) the SMO is rewritten as

$$
\begin{bmatrix} \dot{\hat{v}}_x \\ \dot{\hat{v}}_y \\ \dot{\hat{r}} \end{bmatrix} = \begin{bmatrix} \hat{v}_y r + a_x + \sum_i K_i (v_{x,i} - \hat{v}_x) \\ -\hat{v}_x r + a_y - K_y(t) (a_y - \frac{1}{m} \sum \hat{F}_y) \\ \frac{1}{I_z} \sum \hat{M}_z + K_r(t) \operatorname{sgn}(r - \hat{r}) \end{bmatrix} \tag{7}
$$

where the observer gains are defined according to

$$
\begin{aligned}
K_y &= g_y + \frac{\rho_x}{|a_y - \frac{1}{m} \sum \hat{F}_y| + \eta} \\
K_r &= g_r + \frac{\rho_x}{|r - \hat{r}| + \eta}
\end{aligned} \tag{8}
$$

Thus the SMO can be thought of as the observer in Equation (5) with time-varying gains. How this time-varying gain affects the stability properties is considered next.

IV. Stability properties

The stability analysis for both observers show that they are ISS using Lyapunov analysis. The Lyapunov functions are defined as positive definite functions of the error dynamics

$$
\begin{aligned}
\begin{bmatrix} \tilde{v}_x \\ \tilde{v}_y \\ \tilde{r} \end{bmatrix} &= \begin{bmatrix} v_x - \hat{v}_x \\ v_y - \hat{v}_y \\ r - \hat{r} \end{bmatrix} \\
&= \begin{bmatrix} \tilde{v}_y r - \sum_i K_i (v_{x,i} - \hat{v}_x) \\ -\tilde{v}_x r + K_y (a_y - \frac{1}{m} \sum \tilde{F}_y) \\ \frac{1}{I_z} \sum \tilde{M}_z - K_r (r - \hat{r}) \end{bmatrix}
\end{aligned} \tag{9}
$$

where the the only distinction that will be made between the two observers is the time dependence in K_y and K_r. Furthermore, both observers deploy the Lyapunov function

$$V = \frac{1}{2}(\tilde{v}_x + \tilde{v}_y + \tilde{r}) \tag{10}$$

in the analysis. Assumptions for the stability analysis include

- The wheel speed is positive $v_{x,i} > 0$.
- The friction model defining the wheel model, Equation (3) is continuously differentiable in $x = (v_x, v_y, r)^T$ with bounded partial derivatives.
- The gain for the longitudinal velocity observer is positive $K_i > k_x > 0$.

This section will analyze what separates the two observers, Equations (5) and (7), by looking how their gains are bounded as a result of their stability analysis. The complete proofs are left out to keep the analysis brief.

A. Observer I

The derivative of the Lyapunov function is, Equation (10),

$$\begin{aligned}\dot{V} &\leq -k_x\tilde{x}^2 - K_y c_1 \tilde{v}_y^2 + K_y c_2 |\tilde{r}||\tilde{v}_y| + K_y c_3 |\tilde{v}_x||\tilde{v}_y| \\ &+ c_4\tilde{r}|\tilde{v}_y + c_5\tilde{r}|\tilde{r}| + c_6\tilde{r}|\tilde{v}_x| - K_r\tilde{r}^2 \\ &= -|\tilde{x}|^T A|\tilde{x}|\end{aligned} \tag{11}$$

where

$$A = \begin{bmatrix} k_x & -\frac{1}{2}K_y c_3 & -\frac{1}{2}c_6 \\ -\frac{1}{2}K_y c_3 & K_y c_1 - \frac{1}{2}K_y c_2 - \frac{1}{2}c_4 & \\ -\frac{1}{2}c_6 & -\frac{1}{2}K_y c_2 - \frac{1}{2}c_4 & K_r - c_5 \end{bmatrix} \tag{12}$$

ISS properties can then be showed provided the following bounds on the the observer gains

$$\begin{aligned} K_y &> 0 \\ k_x &> \frac{K_y c_3^2}{4c_1} \\ K_r &> c_5 + \frac{c_7}{4k_x K_y c_1 - (K_y c_3)^2} \end{aligned} \tag{13}$$

For details on the complete proof, see [2].

B. Observer II

The ISS proof for the SMO, [6], follows the same procedure as in [2], albeit with a slightly different result. The bounds on the observer gains (13) are now defined as the intervals

$$\begin{aligned} g_y < K_y < g_y + \frac{\rho_y}{\eta} \\ g_r < K_y < g_r + \frac{\rho_y}{\eta} \end{aligned} \tag{14}$$

The gain will effectively decrease with increasing error between the force and the force estimate, see Equation (14), and decrease otherwise. The gains are time-varying and are be reduced when uncertain force measurements are received. The observer will in sense, believe more in the kinematic model when this happens.

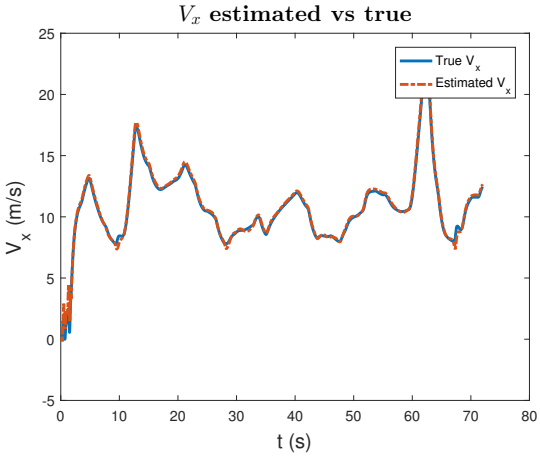

Fig. 2. v_x vs $\hat{v}_x$ using a nonlinear observer.

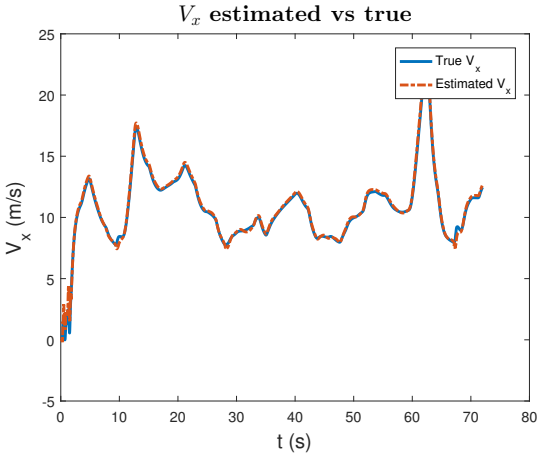

Fig. 3. v_x vs $\hat{v}_x$ using a SMO.

V. Results and Discussion

The results in this section are obtained using the simulation platform CarMaker. This is a platform with an integrated driver that handles a race car optimally around a pre-defined track. Longitudinal velocity, lateral velocity and yaw rate are estimated and plotted against their ground truth from CarMaker, see Figures (2) - (7).

Figures (2) and (3) shows that the estimates of the longitudinal velocities are equal, as expected, for the two observers. This can also be seen from the root mean square error (RMSE) where the two are roughly equal.

Figure (4) shows good tracking of the ground truth signal for lateral velocity except for at the start of the run. During the initial acceleration of the race car, the measurements of a_y oscillate quickly. These oscillations are amplified by the nonlinear observer to larger extent than for the SMO, Figure (5). Another observation is that the nonlinear observer estimates the peaks more accurately then the SMO. Figure (5) shows that the largest peaks, corresponding to the car driving at its limit in turns, are either under- or over-estimated by the SMO. This can be an effect of the variable gain discussed in

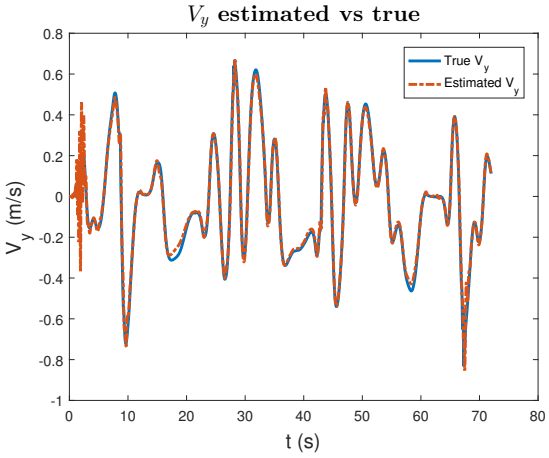

Fig. 4. v_y vs $\hat{v}_y$ using a nonlinear observer.

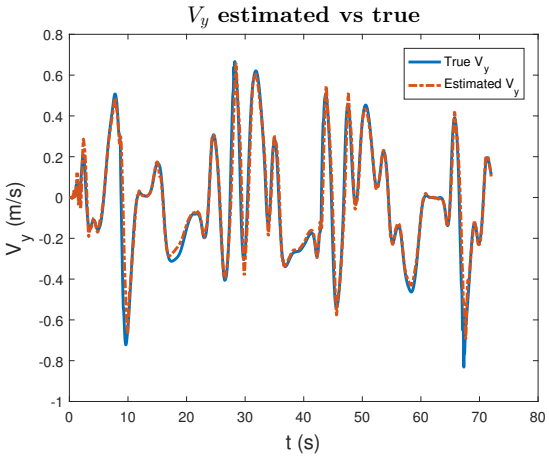

Fig. 5. v_y vs $\hat{v}_y$ using a SMO.

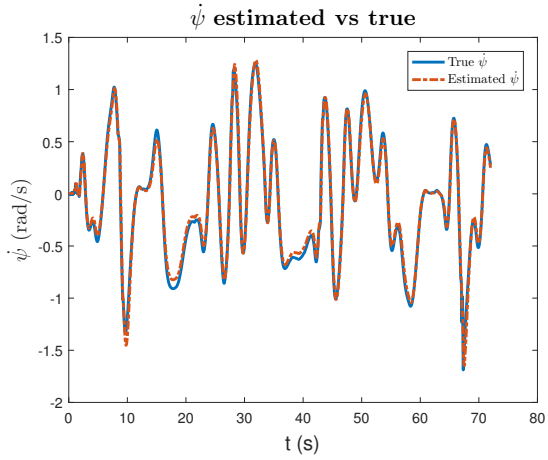

Fig. 6. r vs $\hat{r}$ using a nonlinear observer.

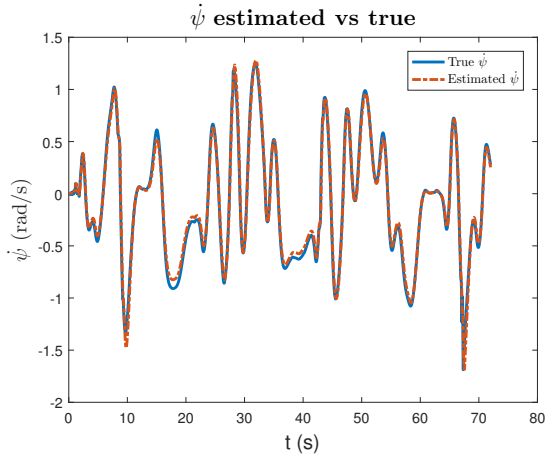

Fig. 7. r vs $\hat{r}$ using a SMO.

Section (IV-B), but its hard to conclude whether this is the reason due to possible sub-optimal tuning. The RMSE values further shows that the SMO performs worse relative to the ground truth velocity despite the large initial oscillations of the nonlinear observers.

The yaw rate appears equal for both observers, both from the plots, Figures (6) and (7), and from the RMSE values. The effect seen in v_y estimates are not observed in this case.

Variable	RMSE$_I$	RMSE$_{II}$
v_x	0.2437	0.2412
v_y	0.0348	0.0687
r	0.0533	0.0546

VI. Conclusion and Further Work

In this work results using two observers for lateral and longitudinal velocities were presented and compared on a simulated Formula Student race car. The results show that both observers provide sufficiently good performance for use in a torque allocation control algorithm. The SMO seems to alleviate fast oscillations in a more acceptable manner than the compared nonlinear observer, but has a worse overall performance. Further work includes testing the observers on an actual Formula Student race car with more realistic noise, integrated with the torque allocation algorithm.

APPENDIX

A. Sum of forces of moments

The force and moment considerations are considered around the center of gravity of the car. Using Newtons second law then gives the following expressions for the forces along the lateral y-axis

$$\begin{aligned}\sum F_y =& F_{x,FL}\sin(\delta_L) + F_{x,FR}\sin(\delta_R) \\ &+ F_{y,FL}\cos(\delta_L) + F_{y,FR}\cos(\delta_R) + F_{y,RL} + F_{y,RR}\end{aligned} \tag{15}$$

The moments around the vertical axis representing yaw motion are obtained in the same fashion

$$\begin{aligned}\sum M_z =& \Big[l_f(F_{x,FL}\sin(\delta_l) + F_{x,FR}\sin(\delta_r)) + l_f(F_{y,FL}\cos(\delta_l) + F_{y,FR}\cos(\delta_r)) \\ &- l_r(F_{y,RL} + F_{y,RR}) + \frac{l_w}{2}\big[(F_{x,FR}\cos(\delta_r) - F_{x,FL}\cos(\delta_l)) \\ &+ (F_{x,RR} - F_{x,RL}) + (F_{y,FL}\sin(\delta_l) - F_{y,FR}\sin(\delta_r))\big]\Big]\end{aligned} \tag{16}$$

Both these are functions of longitudinal and lateral forces calculated with the magic formula, Equation (3), and the measured steering angles δ_L and δ_R.

B. Wheel speeds

The wheel speeds $v_{x,i}$ are computed for each wheel assuming no slip

$$v_{x,i} = R_i^{eff}\omega_i \begin{matrix} + \\ - \end{matrix} \frac{l_w}{2} r \tag{17}$$

where the wheels on the left hand side inherits the minus sign and the right hand side wheels inherits the plus sign.

ACKNOWLEDGMENT

Thanks to Sondre Midtskogen for contributing with development of force estimation and identification of Pacejka parameters.

REFERENCES

[1] W. F. Milliken, "Race car vehicle dynamics," Warrendale, Pa, 1995.

[2] L. Imsland, T. A. Johansen, T. I. Fossen, H. F. Grip, J. C. Kalkkuhl, and A. Suissa, "Vehicle velocity estimation using nonlinear observers," *Automatica*, vol. 42, no. 12, pp. 2091 – 2103, 2006. [Online]. Available: http://www.sciencedirect.com/science/article/pii/S0005109806002780

[3] H. F. Grip, L. Imsland, T. A. Johansen, T. I. Fossen, J. C. Kalkkuhl, and A. Suissa, "Nonlinear vehicle side-slip estimation with friction adaptation," *Automatica*, vol. 44, no. 3, pp. 611 – 622, 2008. [Online]. Available: http://www.sciencedirect.com/science/article/pii/S0005109807003470

[4] J. H. Park and J. H. Kim, "Estimation of vehicle lateral velocity with a nonlinear sliding-mode observer," *IFAC Proceedings Volumes*, vol. 32, no. 2, pp. 8172 – 8177, 1999, 14th IFAC World Congress 1999, Beijing, Chia, 5-9 July. [Online]. Available: http://www.sciencedirect.com/science/article/pii/S1474667017573942

[5] Y. Liu, C. Lin, Z. Xu, and S. Wang, "Sliding mode observers designed to improve observation accuracy of electric vehicle state information," *Energy Procedia*, vol. 105, pp. 4305 – 4311, 2017, 8th International Conference on Applied Energy, ICAE2016, 8-11 October 2016, Beijing, China. [Online]. Available: http://www.sciencedirect.com/science/article/pii/S1876610217310019

[6] L. H. Zhao, Z. Y. Liu, and H. Chen, "Sliding mode observer for vehicle velocity estimation with road grade and bank angles adaptation," in *2009 IEEE Intelligent Vehicles Symposium*, June 2009, pp. 701–706.

[7] H. B. PACEJKA and I. J. M. BESSELINK, "Magic formula tyre model with transient properties," *Vehicle System Dynamics*, vol. 27, no. sup001, pp. 234–249, 1997. [Online]. Available: https://doi.org/10.1080/00423119708969658